First publ. in: Langmuir, The ACS Journal of Surfaces and Colloids 18 (2002), pp. 1082-1090

Concentration Fluctuations in a Model Colloid−Polymer Suspension: Experimental Tests of Depletion Theories

S. Ramakrishnan,[†] M. Fuchs,[‡,||] K. S. Schweizer,[§,†] and C. F. Zukoski*[,†]

Departments of Chemical Engineering, Materials Science and Engineering and Chemistry, and Materials Research Laboratory, University of Illinois, Urbana, Illinois 61801, and Department of Physics and Astronomy, Edinburgh University, JCMB King's Building Mayfield Road, Edinburgh EH9 3JZ, United Kingdom

Received August 6, 2001. In Final Form: November 9, 2001

A light scattering turbidity method has been employed to measure the dimensionless colloidal osmotic compressibility of carefully characterized model athermal colloid (silica)−polymer (polystyrene) suspensions. Mixture thermodynamics is controlled by purely repulsive, hard sphere interactions between the particles while the polymer is in a good solvent. Polymer size is varied by nearly 2 orders of magnitude from far below (1.3 nm) to larger than (70 nm) the particle radius (50 nm). Polymer concentrations are systematically increased up to the solubility limit, and a wide range of colloidal volume fractions up to 0.35 are studied. The measured amplitude of long wavelength colloidal concentration fluctuations provides a sensitive probe of polymer-induced entropic depletion attractions and serves as a demanding test of theoretical descriptions. Quantitative, no adjustable parameter comparisons of experiment with both the classic phantom sphere free volume theory and the recently proposed polymer liquid state integral equation approach reveal systematic deviations. The free volume approach strongly underestimates depletion attraction effects for small polymers and massively overestimates them for large polymers. The direction of the errors of liquid state theory are similar, but much better agreement is found and only modest quantitative errors are present over the entire range of polymer-colloid size asymmetry studied. The importance of physical correlation effects such as fractal coil structure and colloid-induced polymer clustering is deduced. The conclusions based on these homogeneous phase compressibility measurements are consistent with our prior experimental and theoretical studies of phase behavior and polymer insertion chemical potentials.

I. Introduction

The addition of nonadsorbing polymers to colloidal suspensions gives rise to attractions between the particles due to excluded volume effects. Polymer segments in the gap between two particles become increasingly restricted as the particle separation decreases and, as a consequence, lose translational and conformational entropy. This results in a "depletion" of the polymer molecules from the gap and an unbalanced osmotic pressure, which drives the particles together. Depending on the strength and range of these attractive interactions, suspensions gel or undergo liquid/liquid or liquid/crystal phase separation.[1−3] Control of these phase changes is important to achieving desired material properties suited for particular applications where suspension microstructure and mechanical properties are important. Understanding how polymer alters suspension thermodynamic behavior has been based primarily on observations and predictions of phase behavior. The latter typically requires models for particle interactions as well as accurate descriptions of thermodynamic properties of the phases. In this work we report a detailed study of the osmotic compressibility of colloidal spheres of radius R and nonadsorbing polymer (radius of gyration R_g) in which the size asymmetry ratio, R_g/R, is varied from much less than one to greater than one, and as the polymer concentration is increased into the semidilute regime.

The earliest model to describe the depletion effects of nonadsorbing polymer on two-particle interactions was developed by Asakura and Oosawa (AO).[4] In this model, the imbalance in osmotic pressure as polymers are excluded from the gap between the particles results in an effective pair attraction between the colloids. In the AO model, the particles are represented by hard spheres and polymers are treated as spherical objects, without internal (conformational) degrees of freedom, which can pass freely through each other ("phantom spheres") but interact with colloids as hard spheres of radius R_g. Based on the AO potential, Gast et al.[5] developed an effective one-component hard sphere perturbation theory to predict the phase behavior of colloid−polymer mixtures (CPM). Perturbing the hard sphere solution structure with an attractive tail, this theory predicts fluid/fluid and fluid/crystal phase transitions as functions of polymer and particle concentrations and R_g/R. This model correctly captures the transition from stable liquid/liquid transition to metastable liquid/liquid transition as R_g/R drops below ~0.3.

Lekkerkerker et al.[6] extended the above approach by developing a two-component mean field theory based on an AO-like model to predict the phase behavior of CPMs. This approach accounts for polymer partitioning at phase

* Corresponding author.
[†] Department of Chemical Engineering, and Materials Research Laboratory, University of Illinois.
[‡] Edinburgh University.
[§] Department of Materials Science and Engineering, and Department of Chemistry, University of Illinois.
[||] Permanent address: Physik-Department, Technische Universität München, 85747 Garching, Germany.

(1) Pusey, P. N.; Pirie A. D.; Poon, W. C. K. *Physica A* **1993**, *201*, 322.
(2) de Hek, H.; Vrij, A. *J. Colloid Interface Sci.* **1982**, *88*, 258.
(3) Smits, C.; van der Most, B.; Dhont, J. K. G.; Lekkerkerker, H. N. W. *Adv. Colloid Interface Sci.* **1992**, *42*, 33.
(4) Asakura, S.; Oosawa, F. *J. Polymer Sci.* **1958**, *33*, 183.
(5) Gast, A. P.; Hall, C. K.; Russel, W. B. *J. Colloid Interface Sci.* **1983**, *96*, 251. Gast, A. P.; Hall, C. K.; Russel, W. B. *J. Colloid Interface Sci.* **1986**, *109*, 161.
(6) Lekkerkerker, H. N. W.; Poon, W. C. K.; Pusey, P. N.; Stroobants, A.; Warren, P. B. *Europhys. Lett.* **1992**, *20*, 559.

separation and is capable of predicting the coexistence of three phases over a range of polymer and colloid concentrations. In this theory the colloids experience excluded volume interactions with other colloids and polymers that are treated as spheres of radius R_g. Polymer−polymer interactions are ignored.

The Gast et al.[5] and Lekkerkerker et al.[6] theories for phase boundaries and single-phase thermodynamic behavior are fundamentally of the same nature, and in our subsequent discussions we refer to them collectively as "classical" approaches. The approximations by classical theories are more appropriate when the polymer is in a theta solvent, the particles interact as hard spheres, the polymer is dilute, and $R \gg R_g$. As $R_g/R \rightarrow 1$, we expect these classical models to fail qualitatively, as emphasized by the original workers.[5,6] However, the regime of validity of the classical approaches is not known because its simplifications have never been systematically relaxed. Moreover, experimentalists routinely analyze data with the classical models even for $R_g/R \rightarrow 1-2$ [5, 6, 8−11, 13, 14]. Thus, we shall test the predictions of the classical approach over the range of $R_g/R = 0.026-1.4$ studied experimentally in this paper.

Recently, Fuchs and Schweizer[7] developed a modified Percus−Yevick (m-PY) version of the Polymer Reference Interaction Site Model (PRISM) to predict the structure of CPM. PRISM is a two-component liquid state approach, which takes into account polymer structure and correlations on the segment scale, and is, in principle, applicable for all R_g/R ratios and polymer concentrations. Recent m-PY PRISM calculations that employ a Gaussian thread description of polymer chains suggest that the inclusion of many-body correlations is crucial for a successful description of the suspension structures and phase behavior at high colloid densities.[7] Explicit consideration of the conformational entropic contributions of the polymers is required to address the packing of large polymers into the void space between colloidal spheres (or particles into a solution of large polymer molecules). Calculations of the small and wide angle static structure factors of the colloids based on m-PY PRISM were in good agreement with the experimental data of Moussaid et al.[8] in concentrated colloid−polymer mixtures.

While a large number of experimental studies have characterized the phase behavior of colloid polymer mixtures,[9−11] surprisingly few quantitative comparisons have been made with depletion models. Recently we performed a comprehensive study of the phase behavior of a model system,[12] where the particles (silica) interact as hard spheres in the absence of polymer and the polymer (polystyrene) was in good solvent conditions (toluene). The size ratio was varied to cover a range of $0.026 \leq R_g/R \leq 1.4$. A variety of phase transitions, fluid/crystal, fluid/fluid, and gels were observed. The ability of the classical models and PRISM-mPY theory to predict the observed phase behavior was explored. In these studies we use c_p/c_p^* (c_p is the polymer concentration and c_p^* is the polymer overlap, or dilute-semidilute crossover, concentration) as a dimensionless measure of polymer-induced depletion attractions. Our primary finding was that the suspension miscibility improves monotonically as the size asymmetry ratio R_g/R increases (i.e., for larger R_g/R, larger values of c_p/c_p^* are required to drive a phase separation). All classical models of which we are aware predict the opposite trend. However, PRISM/mPY theory predictions for fluid−fluid spinodal phase separation are in agreement with the experimental trends. The success of PRISM can be attributed to the inclusion of important physical factors such as polymer chain structure, polymer−polymer repulsions, physical mesh formation, many-body effective interactions in a true two-component mixture, and colloidal and polymer clustering as a precursor to phase separation. The classical theories generally fail to take these effects into account.

Predicting phase behavior is complicated by the need to have accurate models for thermodynamic properties of two phases. To better understand homogeneous suspension thermodynamics, in this work we focus on the single phase region of the CPM and measure the particle contribution to suspension osmotic compressibility. The ability of the classical theories and PRISM-mPY to predict the measured compressibilites is explored. These comparisons constitute a more rigorous test of the depletion models, as there are no adjustable parameters in comparing theory to experiment (the only required variables are colloid volume fraction ϕ, R_g/R, and c_p/c_p^*), and no additional assumptions about the nature of the phase need to be taken into account. Moreover, the colloidal osmotic compressibility is directly related to the second (concentration) derivative of the free energy and hence is a very sensitive test of theoretical descriptions.

We are aware of only two prior osmotic compressibility studies, and both were on particle systems that were not model hard spheres nor as well characterized as our present work. Weiss et al.[13] used the turbidity method on mixtures of a charged latex (low volume fractions $\phi < 0.1$) and a nonadsorbing, neutral polymer (hydroxy ethyl cellulose) in the good solvent water. The size ratio was $R_g/R \sim 1.1$. This is not an ideal model system to probe the purely excluded volume aspects of depletion interactions since there are Coulombic forces between the colloids but not between the neutral polymer and the latex. Hence, there are strong "nonadditive" effective excluded volume effects present that are absent in our experimental silica based mixture. However, the analysis of these experiments does highlight the strong limitations of classic depletion approaches. The authors employed the AO pair potential multiplied by an empirical fit parameter, q, within an effective one-component description. In conjunction with the random phase approximation (RPA) or atomic mean spherical approximation (MSA) integral equation theory for the scattering function, the colloidal osmotic compressibility data was fitted by varying the parameter q. The value needed to fit the data at low polymer concentrations (below c_p^*) was $q \sim 0.04$, implying a massive factor of ~25 overestimation of the depletion potential by the AO based approach for this R_g/R mixture.

Tong and co-workers[14] used small angle neutron scattering to measure the colloidal osmotic compressibility for low $\phi < 0.12$ suspensions of branched surfactant-coated limestone particles (2 nm radius $CaCO_3$ core, $R \cong 4$ nm) mixed with a single polyolefin polymer under good solvent conditions where $R_g/R \sim 2$. The level to which the particle−

(7) Fuchs, M.; Schweizer, K. S. *Europhys. Lett.* **2000**, *51*, 621. Fuchs, M.; Schweizer, K. S. *Phys. Rev. E.* **2001**, *64*, 021514. Fuchs, M.; Schweizer, K. S. *J. Phys.:Condens. Matter*, submitted.

(8) Moussaid, A.; Poon, W. C. K.; Pusey, P. N.; Soliva, M. F. *Phys. Rev. Lett.* **1999**, *82*, 225.

(9) Ilett, S. M.; Orrock, A.; Poon, W. C. K.; Pusey, P. N. *Phys. Rev. E.* **1996**, *51*, 1344.

(10) Verhaegh, N. A. M.; van Duijneveldt, J. S.; Dhont, J. K. G.; Lekkerkerker, H. N. W. *Physica A* **1996**, *230*, 409.

(11) Vincent, B.; Edwards, J.; Emmet, S.; Croot, S. *Colloids Surf.* **1988**, *31*, 267.

(12) Ramakrishnan, S.; Fuchs, M.; Schweizer, K. S.; Zukoski, C. F. *J. Chem. Phys.* **2001**, in press.

(13) Weiss, A.; Horner, K. D.; Ballauff, M. *J. Colloid Interface Sci.* **1999**, *213*, 417.

(14) Ye, X.; Narayanan, T.; Tong, P.; Huang, J. S.; Lin, M. Y.; Carvalho, B.; Fetters, L. J. *Phys. Rev. E.* **1996**, *54*, 6500.

particle interactions are hard-sphere-like is not well established. These authors fitted their data in a manner similar as that done by Weiss et al.[13] and deduced a value of $q \sim 0.18$ when $c_p < c_p^*$, corresponding to a factor of ~5−6 overestimation of depletion by the classic approach. As $c_p > c_p^*$, the fit parameter q became polymer concentration dependent, decreasing roughly as c_p^{-1}. This contradicts the AO approach but is perhaps not unexpected due to polymer−polymer interactions and screening effects in semidilute solutions.

Hence, very limited prior work hints at strong deviations from the classical approaches when $R \sim R_g$. However, systematic parametric studies were not performed, and the colloids chosen were apparently not model hard spheres. In addition, the prior work considered only rather low colloid volume fractions, which, as we shall demonstrate in this paper, significantly limits the ability to test the predictions of different theories which grow as particle volume fraction increases.

In section II we discuss the theoretical background of the turbidity method used to measure compressibilities, while in section III we discuss the corresponding different model predictions. In section IV experimental methods are described. Comparisons of theory and experiment are given in section V. A brief summary is given and conclusions are drawn in section VI.

II. Theoretical Background of Experimental Method

Structure Factors from Turbidity. The suspensions investigated here are too turbid to carry out angle dependent light scattering to determine structure factors. Instead we employ the method of Ballauff et al.[16−18] to extract the particle osmotic compressibility contribution to the structure factor from the turbidity data. A brief description of the method is given below.

The total intensity of light scattered from a colloid−polymer suspension, $I(q)$, depends on wave vector $q = 4\pi/\lambda \sin(\theta/2)$, where λ is the wavelength of light in the sample and θ is the scattering angle. $I(q)$ contains information on $S_{cc}(q,\phi)$, $S_{pp}(q)$, and $S_{pc}(q)$, the dimensionless colloid−colloid, polymer segment−polymer segment, and colloid−polymer segment partial structure factors, respectively. The relative importance of the latter depends on b_c and b_p, the scattering lengths of the colloid and polymer segment, respectively.

The scattering length scales as the volume of the scattering unit so that for the colloid, $b_c \propto (2R)^3$, while for the polymer, $b_p \propto d^3$, where d is the radius of the monomer. For the silica colloids, $2R = 100$ nm, while an effective diameter of a polystyrene monomer is $d \approx 1$ nm. Thus we estimate $b_p/b_c \approx (1/100)^3 \approx 10^{-6}$. Hence the magnitudes of the polymer−polymer and cross terms in $I(q)$ are negligible and the measured intensity is dominated by the scattering from the colloidal particles.[16]

The turbidity (τ) is defined as the attenuation of the light beam by scattering when passing through a sample

$$\tau = l^{-1} \ln(I_o/I_t) \tag{1}$$

with I_o being the incident intensity of the light, I_t the transmitted intensity, and l the length of the optical path. With the assumption that there is no absorption of the light by the scattering medium, turbidity can be related to the intensity of the scattered light by the following equation:

$$\tau = 2\pi \int_0^\pi R(q) \sin\theta \, d\theta \tag{2}$$

where $R(q)$ is the Rayleigh ratio

$$R(q) \propto c P_{cc}(q) S_{cc}(q,\phi) \tag{3}$$

and c ($= \phi \rho_{silica}$, ρ_{silica} is the particle number density) is the mass concentration of the colloidal particles. In the region of low qR, $P_{cc}(q)$ and $S_{cc}(q,\phi)$ can be approximated by

$$P_{cc}(q) = 1 - \frac{1}{3}(qR)^2 + O(q^4R^4) \tag{4}$$

and

$$S_{cc}(q,\phi) = S(0,\phi) + \gamma(\phi)(qR)^2 + O(q^4R^4) \tag{5}$$

Ballauff et al.[16−18] tested these approximations by comparing the integrated structure factor calculated using the above approximations with the exact result obtained by integrating eq 2 with the Percus−Yevick structure factor. The calculations were carried out for 120 nm diameter hard spheres, and there was good agreement between both methods for wavelengths above 500 nm. Insertion of eqs 4 and 5 into $R(q)$ and subsequent integration of eq 2 leads to

$$\tau \propto c Q(\lambda^2) Z(\lambda^2, c) \tag{6}$$

where $Q(\lambda^2)$ is an integrated form factor and $Z(\lambda^2,c)$ is the integrated structure factor,

$$Z(\lambda^2,c) = S_{cc}(0,c) + O(1/\lambda^2) \tag{7}$$

In the region of low concentrations, $Z(\lambda^2,c) \to 1$ (interparticle interferences are negligible). Hence,

$$\left(\frac{\tau}{c}\right)_{c=0} \propto Q(\lambda^2) \tag{8}$$

and

$$Z(\lambda^2,c) = \frac{(\tau/c)}{(\tau/c)_{c=0}} \tag{9}$$

Equation 9 suggests that $Z(\lambda^2,c)$ can be calculated from a plot of (τ/c) as a function of c at fixed λ by division of the (τ/c) values when the concentration is extrapolated to zero. A plot of $Z(\lambda^2,c)$ as a function of $1/\lambda^2$ is then made, and the intercept of this plot at each concentration is the structure factor $S_{cc}(0,c)$.

III. Model Predictions for Compressibility

A. Classic Free Energy Approaches for Thermodynamic Properties of a CPM. The theory of Lekkerkerker et al.[6] for the thermodynamic properties of CPMs is based on a pseudo two-component description of the suspension free energy. The Helmholtz free energy for a system of N_c colloid particles and N_p polymer molecules in a volume V is written

$$F = F_c(N_c,V) + F_p(N_p,\alpha V) \tag{10}$$

where F_c and F_p are the colloid and polymer contributions

(15) Louis, A. A.; Finken, R.; Hansen, J. P. *Europhys. Lett.* **1999**, *46*, 741.
(16) Horner, K. D.; Topper, M.; Ballauff, M. *Langmuir* **1997**, *13*, 551.
(17) Apfel, U.; Horner, K. D.; Ballauff, M. *Langmuir* **1995**, *11*, 3401.
(18) Weiss, A.; Potschke, D.; Ballauff, M. *Acta Polym.* **1996**, *47*, 333.

to the free energy, respectively. The polymer free energy is coupled to the colloid concentration by determining the chemical potential, or free energy, for inserting a single polymer (approximated as a sphere of radius R_g) in the solution volume not occupied by the particles, V_{free}. Here $\alpha = V_{free}/V$ is the free volume fraction, which depends on the particle volume fraction ϕ and R_g/R. An approximate expression for α was obtained by following Widom's[19] particle insertion method where the chemical potential of a test hard sphere of species M (the polymer) of radius R_g and volume fraction $\phi_M \rightarrow 0$ in a sea of hard spheres (the colloidal particles) of radius R with volume fraction ϕ can be written as

$$\mu_M = \mu_M^0 + kT \log\phi_M - kT \log\alpha \qquad (11)$$

Comparing this expression with the scaled particle expression, or equivalently the Percus−Yevick result, for the chemical potentials of a mixture of hard spheres, one obtains

$$\alpha = (1 - \phi) \exp[-A\gamma - B\gamma^2 - D\gamma^3] \qquad (12)$$

where $\gamma = \phi/(1 - \phi)$, $A = 3\xi + 3\xi^2 + \xi^3$, $B = 9\xi^2/2 + 3\xi^3$, $D = 3\xi^3$, and $\xi = R_g/R$.

The polymer molecules are assumed to be noninteracting, yielding

$$F_p(N_p,\alpha V) = kT\, n_p\, V \log(n_p/\alpha) \qquad (13)$$

where $n_p = N_p/V$. For good solvents (and $R \gg R_g$), this ideal contribution is expected to be valid for $c_p/c_p^* \ll 1$. The colloid contribution to the free energy is given by

$$F_c(N_c,V) = \frac{3kT}{4\pi R^3} V\phi \int \frac{Z_{HS}}{\phi}\, d\phi \qquad (14)$$

where Z_{HS} is the hard sphere compressibility factor.

Once the total free energy is determined, the dimensionless colloid structure factor in the $q \rightarrow 0$ zero angle limit is then given by the formally exact expression[20,21]

$$\frac{1}{S_{cc}(0)} = 1 - \rho_c \frac{C_{cc} - \rho_p N(C_{pp}C_{cc} - C_{pc}^2)}{1 - \rho_p N C_{pp}} \qquad (15)$$

where C_{cc}, C_{pp}, and C_{pc} are the $q = 0$ values of the colloid−colloid, polymer−polymer, and colloid−polymer site−site direct correlation functions. Note that in its dimensionless form, $S_{cc}(q) \rightarrow 1$ as $q \rightarrow \infty$. The direct correlation functions are related to second derivatives of the free energy via the rigorous Kirkwood and Buff[21] relations for binary mixtures

$$C_{cc} = \frac{1}{\rho_c} - \frac{\partial^2(F/VkT)}{\partial\rho_c^2} \qquad (16)$$

$$C_{pp} = \frac{1}{\rho_p N} - \frac{\partial^2(F/VkT)}{\partial\rho_p^2} \qquad (17)$$

$$C_{pc} = -\frac{\partial^2(F/VkT)}{\partial\rho_c\partial\rho_p} \qquad (18)$$

where $\rho_c = N_c/V$ and $\rho_p = N n_p$. Substitution of eqs 16−18 into eq 15 leads to a convenient expression for the inverse dimensionless osmotic compressibility of the colloidal particles in the presence of polymer:

$$\frac{1}{S_{cc}(0)} = \frac{d(\phi Z_{HS})}{d\phi} - \frac{4\pi R^3}{3}\frac{n_p}{\alpha}\phi\frac{d^2\alpha}{d\phi^2} \qquad (19)$$

Predictions of phase behavior of the two-component Lekkerkerker et al.[6] and Gast et al.[5] classical approaches are in good agreement once the volume fraction dependence of the strength of attraction is taken into account.[12] For simplicity, we will compare our experimental results with predictions of eq 19, and refer to it as the "phantom sphere free volume" (PSFV) approach.

B. PRISM. PRISM of the colloid−polymer mixture[7] is a two-component liquid-state approach that takes into account polymer structure and correlations on the segment scale, and therefore is not limited in the range of size ratios and polymer concentrations to which it can be applied. Below is a brief description of how structure factors are (numerically) calculated using PRISM.

The model considers a two-component system consisting of polymers and hard spheres of diameter $\sigma_c (= 2R)$ at a packing fraction ϕ. Polymers are modeled as chains of segments (excluded-volume diameter σ_p) of degree of polymerization N and radius of gyration R_g. The Ornstein−Zernicke-like integral equations for the collective partial structure factors, $\hat{S}_{ij}(q)$, are then written in matrix form as[7,22]

$$\hat{S}^{-1}(q) = \hat{\omega}^{-1}(q) - \rho\,\hat{c}(q) \qquad (20)$$

where $\rho_{ij} = \rho_j\delta_{ij}$, ρ_j are the site number densities, and $c_{ij}(r)$ are the site−site direct correlation functions. The diagonal matrix of intramolecular structure factors, $\hat{\omega}(q)$, contains the colloid element, $\hat{\omega}_c(q) \equiv 1$, and the polymer structure factor, which for analytic simplicity is taken to be of a form appropriate for an ideal or Gaussian random coil.[7] For the pure colloid component, the well-established Percus−Yevick (PY) closure approximation, $c_{cc}(r > \sigma_c) = 0$ is used. For the pure athermal (good solvent conditions) polymer component, the PRISM approach is employed as it has proved versatile and successful for polymers.[22] PRISM considers the segment averaged polymer structure and, in the simplest version, adopts a PY-like closure, $c_{pp}(r > \sigma_p) = 0$.

To close the three coupled integral equations, an approximation for the colloid−polymer direct correlation function is required. Fuchs and Schweizer[7] proposed a novel generalization of the PY closure (referred to as m-PY), motivated by the known physical behavior of polymer packing near a spherical particle. The key idea of the m-PY closure is that it contains a parameter λ_{mPY} that describes the distance from the particle surface over which the polymer conformational entropy is reduced. This length is connected to the depletion attraction range and varies from the polymer size when $R_g \ll R$, to a length of order R when $R_g \gg R$. The inclusion of λ_{mPY} is very important and is needed to address the packing of polymers into the void space between colloidal spheres. λ_{mPY} is also a function of ϕ and c_p/c_p^* due to screening effects. Once λ_{mPY} is determined in a thermodynamically self-consistent manner, the nonlinear integral equations are numerically solved for the structure factors. Details of the solution are given in ref 7.

(19) Widom, B. *J. Chem. Phys.* **1963**, *39*, 2808.
(20) Curro, J. G.; Schweizer, K. S. *Macromolecules* **1991**, *24*, 6736.
(21) Kirkwood, J. G.; Buff, F. P. *J. Chem. Phys.* **1951**, *19*, 774.
(22) Schweizer, K. S.; Curro, J. G. *Adv. Chem. Phys.* **1997**, *98*, 1.

Table 1. Radius of Gyration (R_g) and Polymer Overlap Concentration (c_p*) for the Five Different Polymers Used in This Work[a]

molecular weight (g/mol)	R_g (nm)	R_g/R	c_p* (mg/mL)
2.43×10^3	1.29	0.026	418.79
2.93×10^4	5.74	0.115	57.14
2.124×10^5	18.85	0.377	11.72
5.5×10^5	33.37	0.667	5.47
1.88×10^6	69.77	1.395	2.05

[a] The size ratio R_g/R is also given for each polymer used ($R = 50$ nm).

IV. Experimental Methods

Silica particles were synthesized through base-catalyzed hydrolysis and condensation in ethanol of tetraethylortho silicate (TEOS) at 50 °C following the method of Stober et al.[23] A seeded growth technique[24] was then used to increase particle diameters and suspension weight fraction. Particles were sized using transmission electron microscopy (TEM) and dynamic light scattering, yielding a particle diameter of 100 ± 5 nm. Particles were rendered hydrophobic using the method of Van Helden et al.,[25] which involves boiling of the silica−ethanol mixture with gradual addition of stearyl alcohol. The final boiling process was continued for 6 h at 210 °C, after which the reaction mixture was allowed to cool to room temperature. The particles were washed by dissolving the solid mixture in chloroform followed by centrifugation and decantation. This process was repeated until there was no evidence of residual stearyl alcohol. The particles had a gravimetrically determined density of $\rho_{silica} = 1.9 \pm 0.04$ g/cm^3. Suspensions were prepared by dispersing a known mass of dried silica powder in toluene followed by stirring to better disperse the powder. The volume fractions, ϕ, were also determined by dry weight using $\phi = c/\rho_c$, where c is the mass concentration (mass/volume) of the silica in suspension. In the absence of polymer, sedimentation was not observed for any of the volume fractions used in this work over the time period in which the experiments were done.

Polystyrenes of five different molecular weights, 1.88×10^6, 5.5×10^5, 2.12×10^5, 2.93×10^4, and 2.43×10^3 were purchased from Aldrich Chemical Co. The ratio of the weight average to number average molecular weight is 1.03, implying very monodisperse samples. Static light scattering was used to characterize the 1.88×10^6 MW polymer in toluene. The radius of gyration (R_g) and the second virial coefficient (B_2) were in good agreement with literature values. The good solvent scaling law ($R_g \propto M_w^{3/5}$), confirmed by Berry,[26] was then used to calculate the radii of gyration for the other polymers. The values are shown in Table 1. The polymer overlap concentration, c_p*, was estimated from the standard equation

$$c_p^* = \frac{3M_w}{4\pi R_g^3 N_A} \tag{21}$$

where M_w is the molecular weight of the polymer and N_A is Avogardo's number. The c_p* values are also tabulated in Table 1. For the 1.88×10^6 molecular weight sample, typical uncertainties in the measured R_g are ±10%, implying uncertainties of up to ±30% in the computed values of c_p/c_p*. For the very low molecular weight sample, use of the $R_g \propto M_w^{3/5}$ self-avoiding walk law may be less accurate.

Measurements of turbidity between 500 and 900 nm were conducted using an HP 8453 general purpose UV−visible system thermostated at 35 °C. Initial measurements were done using cuvettes with optical path lengths of 0.2, 0.5, and 1 cm to confirm the Beer−Lambert law. Only data with transmissions between 0.06 and 0.87 were used to determine τ. In all cases, the turbidity was found to be independent of the length of the optical path. All subsequent measurements were done with cuvettes of 1 cm path length.

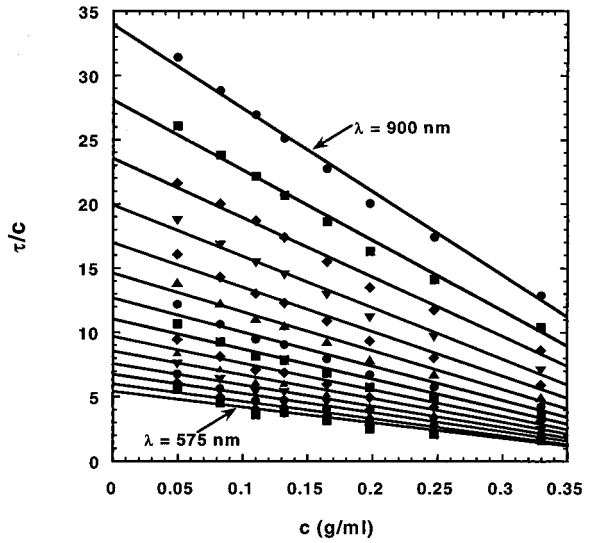

Figure 1. Specific turbidity as a function of concentration for octadecyl silica in toluene without added polymer for different wavelengths. The solid lines are linear curve fits to the data to extract the intercept.

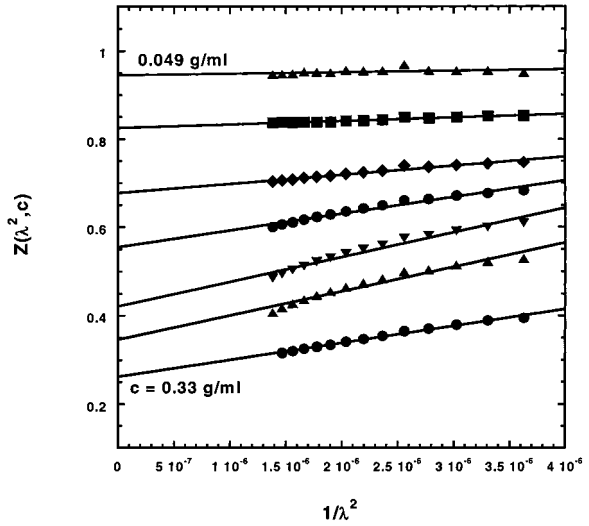

Figure 2. Integrated structure factor of the silica spheres as a function of $1/\lambda^2$ in the absence of polymer for different concentrations. The solid lines are linear curve fits to the data to extract the intercept, which equals the structure factor of the colloidal particles in the zero angle limit ($S_{cc}(0)$).

V. Results and Discussion

Silica spheres coated with octadecanol and suspended in toluene behave as hard spheres[27] above ≅ 30 °C. We chose to work at 35 °C based on compressibility measurements using the turbidity technique. Figures 1 and 2 illustrate this technique by calculating $1/S_{cc}(0,c)$ for the silica spheres suspended in toluene with no added polymer. As discussed in section II, since the diameter of the particles is only 100 nm and wavelengths used are > 500 nm, the approximations (eqs 6 and 7, $qR = 0.88$ for $\theta = 90°$) used in this technique are justified. Shown in Figure 3 is a plot of $1/S_{cc}(0)$ (triangles) for the silica spheres as a function of volume fraction ϕ and compared with the

(23) Stober, W.; Fink, A.; Bohn, E. *J. Colloid Interface Sci.* **1968**, *26*, 62.
(24) Bogush, G. H.; Tracy, M. A.; Zukoski, C. F. *J. Non-Cryst. Solids* **1988**, *114*, 95.
(25) van Helden, A. K.; Jansen, J. W.; Vrij, A. *J. Colloid Interface Sci.* **1981**, *81*, 354.
(26) Berry, G. C. *J Chem. Phys.* **1966**, *44*, 4550.
(27) Rutgers, M. A.; Dunsmuir, J. H.; Xue, J. Z.; Russel, W. B.; Chaikin, P. M. *Phys. Rev. B* **1996**, *53*, 5043.

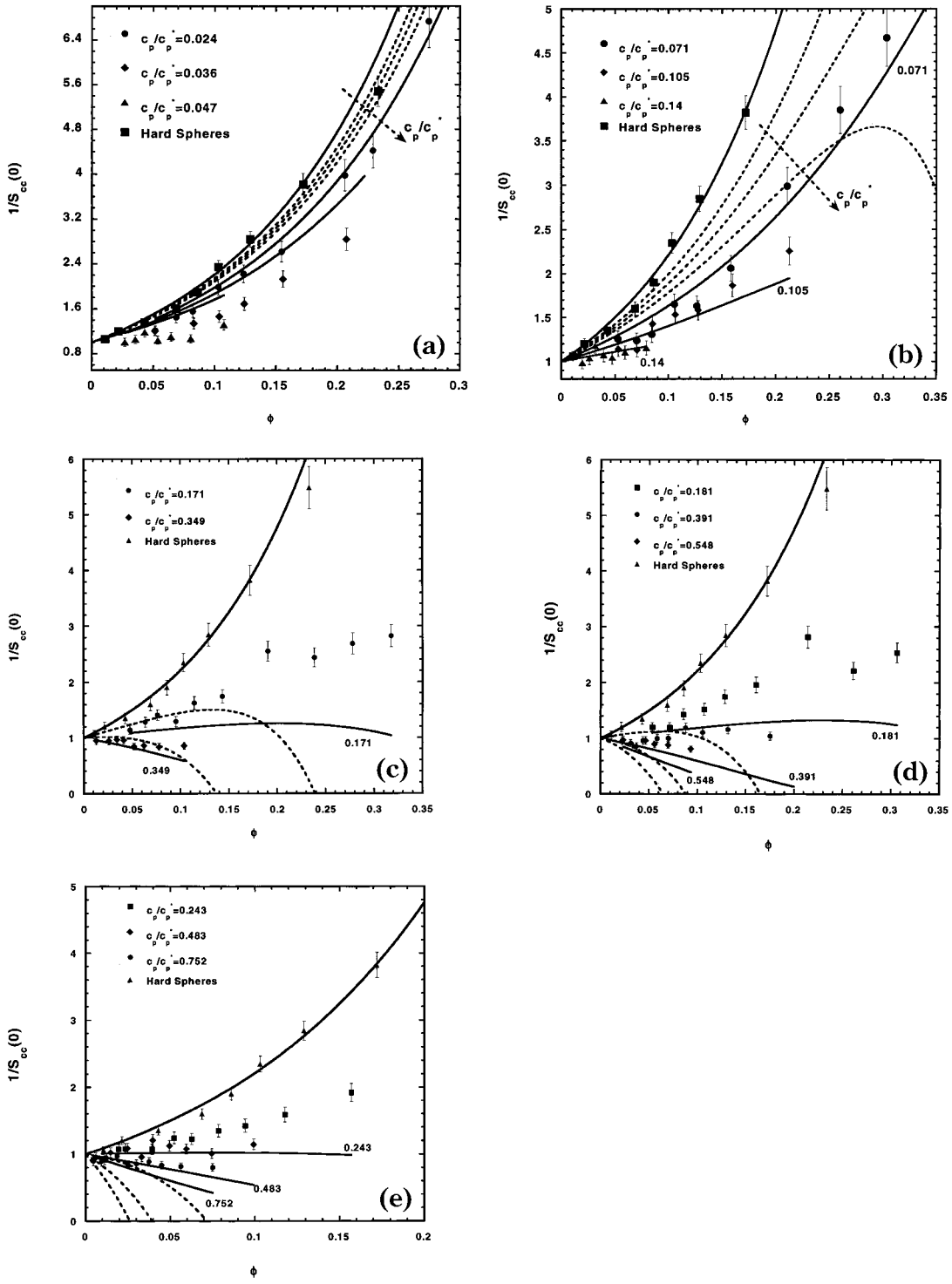

Figure 3. (a−e) Inverse dimensionless osmotic compressibility of the colloidal particles as a function of colloid volume fraction for different polymer molecular weights (size ratios R_g/R) and reduced polymer concentrations. The solid symbols are the experimental points for different polymer concentrations. The uppermost data points correspond to silica in toluene with no added polymer (hard spheres), and the solid curve through them is the Carnahan Starling equation of state. The other solid curves are calculations of PRISM m-PY and the dashed curves are calculations of the phantom sphere free volume model[6] for the experimental values of c_p/c_p^*. (a) 2.43×10^3 g/mol ($R_g/R = 0.026$); (b) 2.93×10^4 g/mol ($R_g/R = 0.115$); (c) 2.124×10^5 g/mol ($R_g/R = 0.377$); (d) 5.5×10^5 g/mol ($R_g/R = 0.667$); (e) 1.88×10^6 g/mol ($R_g/R = 1.395$).

Carnahan−Starling equation of state.[28] Comparison of experimental and theoretical data requires converting c to ϕ. In our case, the comparison is made with the gravimetrically determined value of ρ_{silica} of 1.9 g/cm^3. The agreement with no adjustable parameters is strong evidence that the particles in the absence of polymer interact as hard spheres.

The phase diagram of the hard sphere silica particles in the presence of polystyrene of five different molecular weights has been previously determined.[12] The results are shown in Figure 4 where phase diagrams are plotted

(28) Hansen, J. P.; McDonald, I. R. *Theory of Simple Liquids*, 2nd ed.; Academic Press: London, 1986.

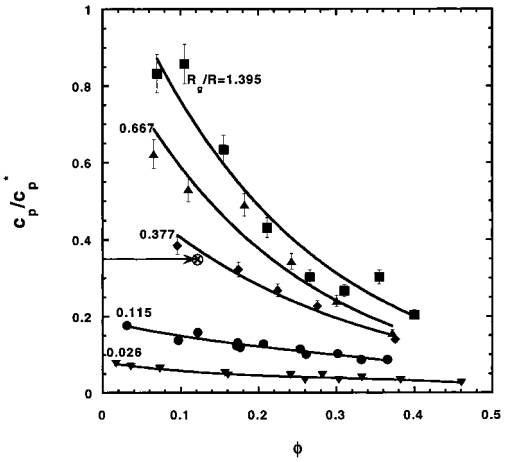

Figure 4. Experimental phase diagram of silica in toluene in the presence of polystyrene for five different values of R_g/R. The horizontal axis is the colloid volume fraction ϕ and the vertical axis is the dimensionless polymer concentration (c_p/c_p^*). The curves are drawn to guide the eye. The arrow depicts the path taken in the measurement of osmotic compressibility at c_p/c_p^* of 0.35 for $R_g/R = 0.377$.

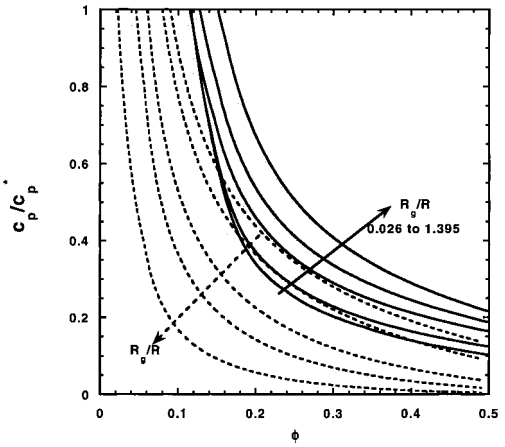

Figure 5. Fluid−fluid spinodals calculated from the PRISM/m-PY theory (solid curves) and the phantom sphere free volume theory (dashed curves) for the R_g/R values of the experiments: $R_g/R = 0.026$, 0.115, 0.377, 0.667, and 1.395.

in terms of a dimensionless polymer concentration c_p/c_p^* as a function of the colloid volume fraction ϕ. When R_g/R is 0.026, the points indicate the formation of a homogeneous "gel". When R_g/R is 0.115, the suspension separates into a dense lower phase and a dilute upper phase. We suspect this lower phase to consist of crystals, but this has not yet been confirmed with X-ray scattering. For the three higher molecular weights, the phase boundary is clearly a liquid/liquid phase separation. More experimental details and comparisons with theory of the measured phase behavior are described elsewhere.[12] As discussed above, Figure 4 demonstrates that the suspension miscibility monotonically improves as the size asymmetry ratio R_g/R increases (i.e., larger values of c_p/c_p^* are required to produce two phases as R_g/R increases), which disagrees with the predictions of classic theories but agrees with PRISM/mPY theory (see Figure 5).

The curves shown in Figure 4 are drawn to guide the eye. Below the curves, there is a single phase region while (for $R_g/R \geq 0.115$) phase separation occurs as the curves are crossed. Once the phase diagram of the colloidal silica in the presence of the polymers was determined, the osmotic compressibility measurements were made for each polymer molecular weight at different polymer concentrations up to the solubility (or gel) point. The different conditions used in the measurements are listed in Table 2. To illustrate our approach, the path taken in measurement of the osmotic compressibility at $c_p/c_p^* = 0.35$ for $R_g/R = 0.377$ is depicted by the arrow in Figure 4. The colloid concentration is varied from dilute to near the point on the solubility boundary, which is shown by the symbol ⊗.

Table 2. Conditions Used in the Experimental Measurements of Osmotic Compressibility[a]

R_g/R	c_p/c_p^* expt	c_p/c_p^* PRISM
0.026	0.023	0.023
	0.036	0.07
	0.047	0.10
0.115	0.071	0.071
	0.105	0.105
	0.140	0.14
0.377	0.170	0.11
	0.349	0.30
0.667	0.181	0.10
	0.391	0.20
	0.548	0.30
1.4	0.243	0.125
	0.483	0.24
	0.752	0.35

[a] The last column gives the estimated polymer concentration one needs to use in PRISM theory to quantitatively fit the experimental data. The uncertainties in the calculated experimental values of c_p/c_p^* could be as large as 30%.

The results of the osmotic compressibility measurements are presented in Figure 3a−e. Shown in each graph is the silica in pure toluene (hard spheres) result for purposes of comparison. Upon addition of polymer, the experimental points shift downward, indicating the presence of polymer-induced depletion attractions. The solid lines in Figure 3a−e are comparisons with PRISM theory, and the dashed lines are the classic PSFV results. There are no adjustable parameters in these comparisons. The only required variables are c_p/c_p^* and R_g/R, which are known experimentally, although possible uncertainties of order ±30% and ±10%, respectively, should not be forgotten.

For R_g/R of 0.026 (Figure 3a), both the PSFV and PRISM theories underpredict the strength of depletion attraction, with the classic approach predicting much weaker depletion effects. The same trend is also seen in the phase behavior where the theoretical models underpredict the strength of depletion attraction.[12] Figure 5 shows the spinodal curve predictions of the PSFV and PRISM theories for the experimentally relevant values of R_g/R. Note that for $R_g/R = 0.026$, the PRISM spinodal lies below the classical result, consistent with its prediction of larger colloidal osmotic compressibility. When R_g/R is 0.115 (Figure 3b), PRISM essentially quantitatively predicts the inverse osmotic compressibility right up to the solubility point, while the PSFV model underpredicts the strength of depletion attraction (in agreement with phase diagram predictions[12]). For the higher molecular weights (Figure 3c−e) with $R_g/R = 0.667$ and 1.395, both PRISM and the classical model overpredict the strength of depletion attractions, with PRISM now showing the weaker depletion effect. However, the predictions of PRISM theory are much closer to the experimental data than those of the classical theory, especially as R_g/R and/or ϕ increase.

At low R_g/R values, the PSFV model strongly underpredicts the strength of depletion, while at higher R_g/R values it strongly overestimates the strength of depletion. Hence one would expect that the PSFV model may give

(fortuitously) good predictions at intermediate values of R_g/R. The data in Figure 3 suggest this occurs near $R_g/R \approx 0.3$. More importantly, the comparisons in Figure 3 suggest the classical approach incurs (at least) two significant errors of a qualitatively different nature depending on whether $R_g \ll R$ or $R_g \gg R$. To a far smaller extent, the same is true of the PRISM/mPY theory.

The comparisons in Figure 3 involve no adjustable parameters since c_p/c_p^* and R_g/R are known experimentally, at least to within tolerances of ~30% and 10%, respectively. It is an interesting question whether the theories can quantitatively account for the data if one uses R_g/R or c_p/c_p^* as a single adjustable parameter. An answer of "yes" suggests the theory does capture the essential physics but incurs errors of a quantitative nature. Here we investigate this question based on adjusting c_p/c_p^* as done previously by others,[13−15] but our basic conclusions would not change if instead R_g/R was varied.

Figure 6a,b are a representative result for $R_g/R = 0.667$. One sees that PRISM theory can account, essentially quantitatively, for the data if c_p/c_p^* is reduced by a single factor of ~2 for all ϕ. However, the PSFV theory cannot be forced to fit the data for all colloid volume fractions and displays a qualitatively incorrect shape. We have carried out such comparisons for all five samples but refrain from presenting the many more plots since our conclusions are the same for all R_g/R values. Table 2 summarizes our findings for PRISM theory, and Figure 7 provides an additional explicit example for the smallest polymer case. As seen from Table 2, a reduction (increase) of c_p/c_p^* by a factor of ~2 (2) is required for $R_g/R = 0.667$ and 1.395 (0.026). For the $R_g/R = 0.115$ sample, the PRISM predictions are essentially exact to within the experimental uncertainties. Hence, consistent with our prior phase diagram study[12] and limited prior comparisons to scattering data,[7,8] we conclude that PRISM theory is much more accurate than the classic type approach for describing polymer-induced long-wavelength colloidal concentration fluctuations.

We now turn to the question of physical interpretation of our findings. The classic approaches treat polymers as structureless hard spheres that can pass through each other. This contrasts with PRISM theory which accounts for chain connectivity and intermolecular excluded volume interactions. In the $R_g \ll R$ colloidal regime, the classic approaches predict weaker depletion attraction than PRISM theory as manifested in the polymer insertion chemical potential,[7,12] the spinodal boundary[12] (see Figure 5), and the homogeneous phase osmotic compressibility. A possible physical origin of the differences is that the classic approaches ignore polymer density fluctuations due to conformational degrees of freedom. The latter are expected to also be restricted (in addition to translational entropy), or equivalently the orientational (rotational) freedom of polymer coils is reduced, by the presence of colloids. Hence, stronger depletion attractions in PRISM theory relative to AO model based approaches might be expected. Interpretation of the fact that PRISM appears to quantitatively underestimate depletion attraction relative to experiments for $R_g/R = 0.026$ is subtle. This is perhaps a not unexpected consequence of errors incurred by the inevitable closure approximations in liquid state theory, which are expected on theoretical grounds to be largest when $R \gg R_g$ and low ϕ.[7] On the other hand, for the $R_g/R = 0.026$ system the polymer size is not much larger than the styrene monomer diameter; hence, the use of the infinitely thin "thread" polymer model in the present implementation of PRISM theory is expected to incur quantitative error.

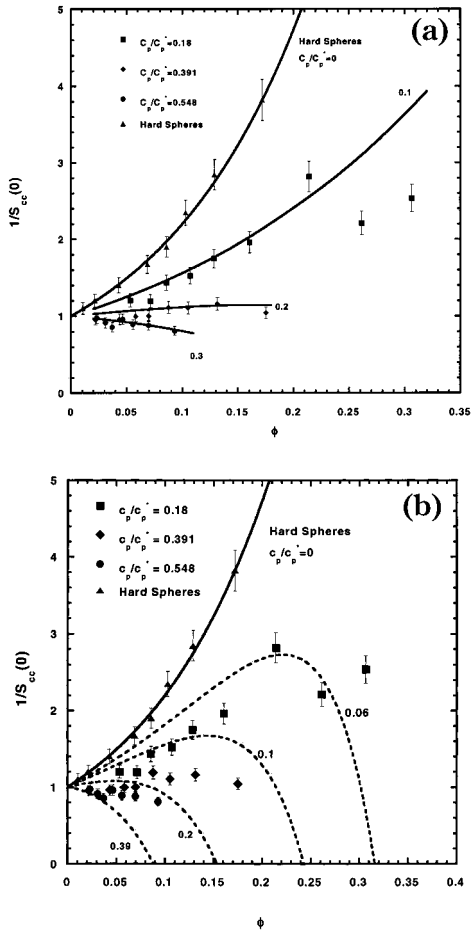

Figure 6. (a,b) Inverse dimensionless osmotic compressibility of colloidal silica in the presence of 5.5×10^5 g/mol mwt polystyrene in toluene ($R_g/R = 0.667$). The solid symbols are the experimental points. The solid and dashed curves are calculations from (a) m-PY PRISM and (b) phantom sphere free volume model, respectively, for values of c_p/c_p^* given alongside each curve. The value of c_p/c_p^* is adjusted to test the validity of the models in predicting the shape of the experimental data.

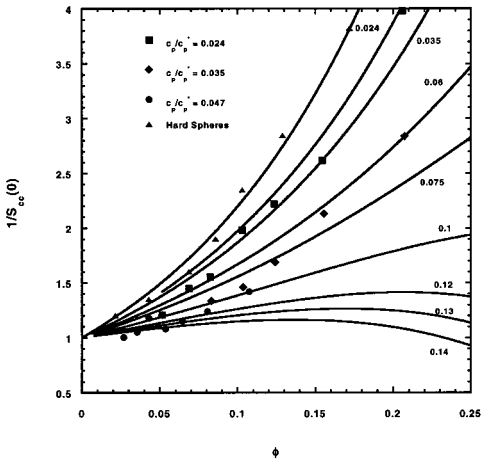

Figure 7. Inverse dimensionless osmotic compressibility of colloidal silica in the presence of 2.43×10^3 g/mol mwt polystyrene in toluene ($R_g/R = 0.026$). The solid symbols are the experimental points. The curves are calculations from m-PY PRISM for values of c_p/c_p^* given alongside each curve. The value of c_p/c_p^* is adjusted to test the validity of the model in predicting the shape of the experimental data.

In the regime R_g of order or greater than R, the classic approaches massively overestimate depletion attractions

as manifested in the polymer insertion chemical potential,[7,12] spinodal boundaries,[12] and colloid osmotic compressibility. The origin of this failure seems obvious: representation of an (open) polymer coil by a solid particle is qualitatively inappropriate as expected by prior workers.[5,6] In this regime, PRISM theory also appears to overestimate depletion attraction, but in a modest, quantitative manner. This we believe is at least partially due to the use of an effective Gaussian coil model under athermal conditions instead of the correct self-avoiding walk (SAW) polymer statistics. The latter corresponds to a more swollen, less dense structure, which would allow easier penetration of the polymer coil by particles. The use of a more internally dense ideal coil model would then suppress particle penetration, and thereby enhance depletion attraction. This error of PRISM theory is of a purely technical nature, and can be relaxed by resorting to a more elaborate numerical approach required to treat a SAW.

One might ask whether the difficulties of the classical PSFV approach can be resolved by using the more realistic PRISM expression for the insertion chemical potential in eqs 11 and 12. However, we have previously shown[12] that for the present range of R_g/R ratios studied experimentally, the differences between PRISM predictions for the fractional free volume and eq 12 are rather small. They cannot account for the qualitative errors made by the PSFV approach for fluid/fluid phase separation boundaries, and hence the critical importance of nonzero polymer concentration was established.

More generally, the classic approaches do not account for multiple physical effects that are taken into account by PRISM theory. These include (1) polymer−polymer repulsions in good solvents which increase in importance as c_p/c_p^* and/or R_g/R increase, (2) many-body effects (non pair decomposable depletion attraction), which tend to reduce depletion effects, and (3) local and long distance changes in colloid structure and free volume distribution, and polymer−polymer correlations, at nonzero polymer concentrations which will depend on R_g/R, c_p/c_p^* and ϕ.

The interpretations advanced above are consistent not only with our present findings for the osmotic compressibility, but also our prior detailed comparisons of theory and experiment for phase boundaries.[12]

Finally, to assess the ability of simple pair potentials to predict the osmotic compressibility, the adhesive hard sphere[29] (AHS) and the square well potential[30] were used to calculate $1/S_{cc}(0)$ for the experimental conditions used in this work. These pseudo one-component models are often used to describe colloid suspension thermodynamics as their ease of application makes them very attractive. Usually for these models, results are available from integral equation theory or computer simulations, which include colloidal many-body effects. Details of the mapping based on forcing agreement between AO second virial coefficients and AHS and square well equations of state are given elsewhere.[12] We refrain from presenting more figures, and simply summarize our findings. The main conclusions from these comparisons are two-fold. (1) For small polymers, $R_g/R = 0.026$ and 0.115, the predictions are of comparable accuracy as PRISM theory. (2) However, the comparisons systematically worsen as R_g/R increases and the strength of the depletion attraction is severely overpredicted in a manner resembling the PSFV approach. These calculations reinforce our prior conclusion, based on detailed study of phase diagrams,[12] that replacing the CPM with a one-component particle fluid is not adequate and can incur qualitative errors as $R_g \rightarrow R$ due to the inadequacy of an effective pair decomposable depletion potential approximation for mimicking the polymer component.

(29) Baxter, R. J. *J. Chem. Phys.* **1968**, *49*, 2770.
(30) Ramakrishnan S.; Zukoski, C. F. *J. Chem. Phys.* **2000**, *113*, 1237.

VI. Summary and Conclusions

In this work we have experimentally studied the single-phase colloidal osmotic compressibility of a model athermal polymer−colloid suspension over a wide range of size asymmetry, colloid volume fraction, and polymer concentration. Our results reinforce the conclusions drawn in earlier work based on the phase behavior of these suspensions.[12] The phantom sphere free volume approach underpredicts the depletion attraction effects at small R_g/R, and severely overpredicts them at larger R_g/R. Even if c_p/c_p^* is treated as an adjustable parameter, classical approaches do not capture the volume fraction dependence of the compressibility at elevated ϕ. PRISM theory is very successful in predicting the compressibility curves if c_p/c_p^* is taken as an adjustable parameter. More importantly, it is quantitative or semiquantitative for all R_g/R values based on no adjustable parameter comparisons, although modest systematic deviations from the data are apparently present at low and high R_g/R values. The critical role of nonzero polymer concentration, and the thermodynamic state and R_g/R ratio dependent corrections to polymer-mediated depletion interactions, absent in classic approaches, can thereby be deduced.

Acknowledgment. Work at Illinois was supported by the U.S. Department of Energy Division of Materials Science Grant No. DEFG02-91ER45439 through the Frederick Seitz Materials Laboratory. M.F. was supported by the Deutsche Forschungsgemeinschaft under Grant No. Fu 309/3 and through the SFB 563.

LA0112458